Supramolecular Chemistry Hot Paper

International Edition: DOI: 10.1002/anie.201901833
German Edition: DOI: 10.1002/ange.201901833

Molecular Swings as Highly Active Ion Transporters

*Changliang Ren, Feng Chen, Ruijuan Ye, Yong Siang Ong, Hongfang Lu, Su Seong Lee, Jackie Y. Ying, and Huaqiang Zeng**

Abstract: *Ions are transported across membrane mostly via carrier or channel mechanisms. Herein, a unique class of molecular-machine-inspired membrane transporters, termed molecular swings is reported that utilize a previously unexplored swing mechanism for promoting ion transport in a highly efficient manner. In particular, the molecular swing, which carries a 15-crown-5 unit as the ion-binding and transporting unit, exhibits extremely high ion-transport activities with EC_{50} values of 46 nM (a channel:lipid molar ratio of 1:4800 or 0.021 mol% relative to lipid) and 110 nM for K^+ and Na^+ ions, respectively. Remarkably, such ion transport activities remain high in a cholesterol-rich environment, with EC_{50} values of 130 (0.045 mol% relative to lipid/cholesterol) and 326 nM for K^+ and Na^+ ions, respectively.*

Molecular transport across membrane is predominantly mediated by either carriers[1] or channels.[2] Carriers do not span the entire hydrophobic membrane region, often undergo dramatic conformational changes before and after binding to the molecular species and mediate molecular transport via an intermittent transport pathway. In contrast, channel molecules form a well-defined transmembrane pathway that is open to both the intra- and extracellular environments, thus enabling molecules to rapidly diffuse through membrane without interruption. We describe here an alternative swing mechanism for achieving exceptionally efficient ion transport. This swing mechanism blurs the boundaries between carrier and channel mechanisms. Like carriers, molecular swings are not simultaneously open to both the intra- and extracellular environments. Like channels, molecular swings do follow a defined pathway for facilitated molecular transport.

Our design of molecular swing is largely inspired by the recent burgeoning developments in the field of artificial molecular machines,[3] which attempt to mimic macroscopic functions using molecules at the microscopic level. Researching novel molecular machines is an active area at the forefront of chemical sciences, with the 2016 Nobel Prize in Chemistry awarded to Jean-Pierre Sauvage,[4a] Sir J. Fraser Stoddart,[4b] and Bernard L. Feringa.[4c] Despite the availability of diverse types of molecular machines for performing versatile functions seen in the macroscopic world (for example, rotors,[5a–e] synthesizers,[5f,g] pumps,[5h,i] muscles,[5j,k] walkers,[5l] and movers[5m]), the corresponding applications in facilitating molecular transport across a membrane have remained essentially unexplored. The only example we are aware of uses a rotaxane to transport ions via a shuttling mechanism.[6] Having an EC_{50} value of only 1.0 μM (3.0 mol% relative to lipid), its activity is very low.

In line with our long-standing interests in membrane transporters[7] and stimulated by the macroscopic swings, one of the simplest and perhaps most fun outdoor activities for kids, we wondered whether we could build similar objects at the molecular level, with a swing function, to operate within the context of cell membrane. As illustrated in Figure 1a, analogous to the macroscopic swing, the nanoscale-sized molecular swing was designed to contain all four essential structural elements with the appropriate dimensions: two hydroxyl-rich cholesterol groups as the lag bolts (or lipid anchors), one linear hydrazide segment as the cross-beam, one flexible PEG chain as the rope, and one crown ether as the swing seat. The two lag bolts allow the molecular swing to firmly anchor into the hydrophilic membrane regions that serve as the support beams. A minor difference does exist between the macroscopic and molecular swings: while the former swings in the direction perpendicular to the cross-beam, the swing direction in the latter is expected to be mostly parallel to the cross-beam. The ability of the crown ethers to bind Na^+ and K^+ ions should endow these artificial molecular swings with the ability to swing ions across a membrane in the presence of an ionic concentration gradient.[7b]

To evaluate the hypothesis regarding the swing mechanism, two molecular swings containing 15-crown-5 (**MS–C5**) or 18-crown-6 (**MS–C6**) units as the swing seat were synthesized. Their ion-transport activities were assessed using the well-established 8-hydroxypyrene-1,3,6-trisulfonic acid (HPTS) assay. In this assay, a pH-sensitive HPTS dye whose fluorescence increases with increasing pH was placed inside egg yolk L-α-phosphatidylcholine (EYPC)-based large unilamellar vesicles (LUVs) to monitor ion-transport-induced changes in intravesicular pH and fluorescence intensity of the HPTS dye (Figure 2a). With a a pH gradient of 7 to 8 applied across LUVs, high ion-transport activities recorded over a period of 300 s were always accompanied by large increments in the ratiometric value of HPTS fluorescence at 460 and 403 nm. After subtracting the background intensity, the ratiometric values were further normalized, with that induced by Triton X-100 (added at $t = 300$ s) set as 100%, and used to gauge the ion-transport ability of ion transporters in terms of fractional transport activity.

[*] Dr. C. Ren, Dr. F. Chen, Dr. H. Lu, Prof. Dr. J. Y. Ying, Dr. H. Zeng
NanoBio Lab
31 Biopolis Way, The Nanos, Singapore 138669 (Singapore)
E-mail: hqzeng@nbl.a-star.edu.sg
R. Ye
Department of Chemical and Biomolecular Engineering,
National University of Singapore, Singapore 117585 (Singapore)
Dr. Y. S. Ong, Dr. S. S. Lee
Institute of Bioengineering and Nanotechnology
31 Biopolis Way, The Nanos, Singapore 138669 (Singapore)
Supporting information and the ORCID identification number(s) for the author(s) of this article can be found under: https://doi.org/10.1002/anie.201901833.

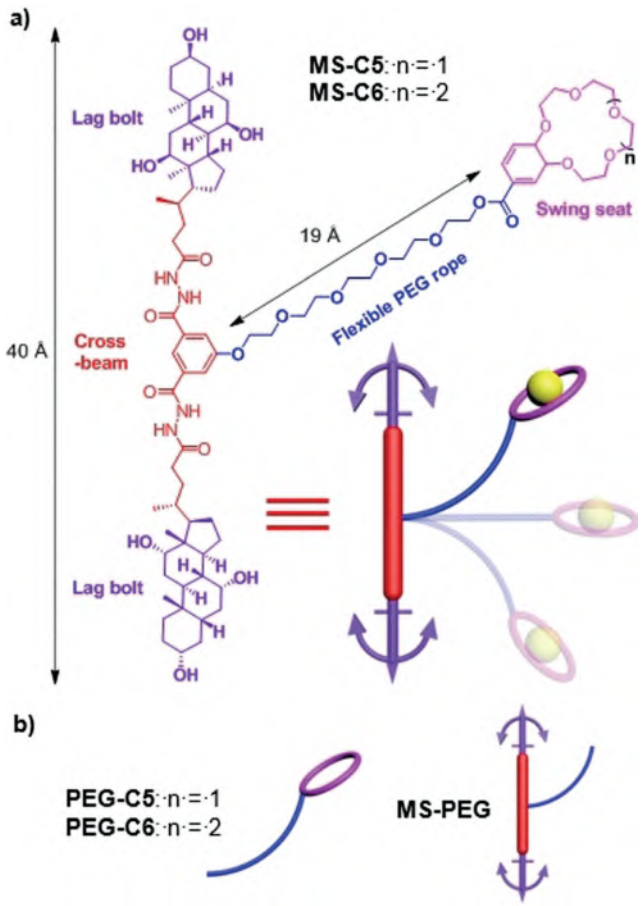

Figure 1. a) Chemical structure of molecular swings **MS–C5** and **MS–C6**, which carry four essential structural elements, including lag bolts to allow the swings to anchor into the hydrophilic membrane regions and a swing seat for binding and transporting metal ions. For a computationally optimized structure of **MS–C5**, see Figure S1 in the Supporting Information. b) Three control compounds **PEG–C5** and **PEG–C6**, which contain only the PEG rope and the swing seat, and **MS–PEG**, which contains all components except for the swing seat, for comparison with **MS–C5** and **MS–C6**.

Using this assay, both molecular swings (**MS–C5** and **MS–C6**) displayed distinctively high efficiencies of 81–98% in transporting Na^+ and K^+ ions at a low concentration of 1 μM (Figure 2b). In sharp contrast, the transport of either Na^+ or K^+ ions by the three control compounds, **MS–PEG** that lacks a swing seat as well as **PEG–C5** and **PEG–C6** that contain only a swing seat and a flexible PEG chain, were negligible even at a high concentration of 5 μM with respect to the background signals. Similarly, a control compound (**C14-Crown 5**, Supporting Information, Figure S6), bearing a hydrophobic $C_{14}H_{29}$ chain, showed very low activities with EC_{50} values of 23.9 μM and 10.1 μM for Na^+ and K^+ ions, respectively.

Interestingly, although ion-transport activities toward both Na^+ and K^+ ions differ only slightly between **MS–C5** and **MS–C6** at 1 μM, such activities decrease more sharply for **MS–C6** than **MS–C5** at lower concentration ranges. More specifically, **MS–C5** at just 80 nM could transport K^+ ions as fast as **MS–C6** at 250 nM (Figure 2c). More detailed studies of various extravesicular alkali metal salts MCl ($M^+ = Li^+$, Na^+, K^+, Rb^+, and Cs^+) demonstrated that **MS–C5** is not only more capable but also more selective in transporting K^+ ions across membrane than **MS–C6**. Using the Hill analysis, the EC_{50} values at which the transporters reach 50% ion-transport activity were determined to be 141, 110, 46, 108, and 207 nM for Li^+, Na^+, K^+, Rb^+, and Cs^+ ions, respectively, for **MS–C5** (Figure 2d and Supporting Information, Figure S2 and S3). In comparison, EC_{50} values for transporting Na^+ and K^+ ions were 172 and 101 nM, respectively, for **MS–C6** (Supporting Information, Figure S4), and 2.91 μM and 101 nM, respectively, for valinomycin (Supporting Information, Figure S5). At the EC_{50} value of 46 nM, a channel:lipid molar ratio was calculated to be 1:4800 (or 0.021 mol% relative to lipid), signifying the extremely active nature of **MS–C5**-mediated transport of K^+ ions. Remarkably, these ion-transport activities remain high in lipids containing 33 mol% cholesterol, with EC_{50} values of 130 nM (0.045 mol% relative to lipid/cholesterol) and 326 nM for K^+ and Na^+ ions, respectively (Supporting Information, Figure S7).

To ascertain that the observed ion transport did result from ion-transporting function of these molecular swings, rather than from their possible membrane-lysing activity, a carboxyfluorescein-leakage assay ($\lambda_{ex} = 492$ nm, $\lambda_{em} = 517$ nm) was conducted (Supporting Information, Figure S8). Melittin, which can form a pore greater than 1 nm in size (a size that is larger than carboxyfluorescein) in membrane or efficiently lyse the membrane at low concentrations, caused large increases in fluorescence of 59% and 92% at 100 nM and 200 nM, respectively, while **MS–C5** produced a change of only 2% at 1 μM. These data conclusively establish membrane integrity in the presence of the molecular swing **MS–C5**.

Next, chloride-sensitive SPQ dye (6-methoxy-*N*-(3-sulfopropyl) quinolinium) was introduced into the assay, with the intravesicular region containing 0.5 mM SPQ dye and 200 mM $NaNO_3$, and the extravesicular region containing 200 mM NaCl (Figure 3a). In contrast to the anion channel **L8**,[7b] which results in fluorescence quenching of SPQ by 46% at 1 μM, no detectable fluorescence quenching was observed with **MS–C5**, indicating that the latter is incapable of transporting anions, such as chlorides, along its linear backbone composed of lag bolts and a hydrazide segment. These results support the H^+/M^+ antiport as the main transport mechanism of **MS–C5**. Similar results were also observed for **MS–C6** (Supporting Information, Figure S9a).

To compare the relative transport rates of K^+ and H^+ ions, the HPTS assay was performed with extravesicular KCl at 100 mM in the presence of a potent proton carrier **FCCP** (Figure 2a and Figure 3b). If the transport rate of H^+ is much slower than that of K^+, **FCCP** will help to increase the transport rate of H^+ to accompany the molecular-swing-mediated rapid influx of K^+, giving rise to a significant increase in fluorescence intensity. Experimentally, we did observe a net increase of 17% between transport activities mediated by **MS–C5** alone (74%) and **MS–C5** in the presence of **FCCP** (57%). This increase, when compared to a small change of 3% between **FCCP** alone and background signal, is significant enough for one to conclude that K^+ ions are transported much faster than H^+ ions. Replacing extravesic-

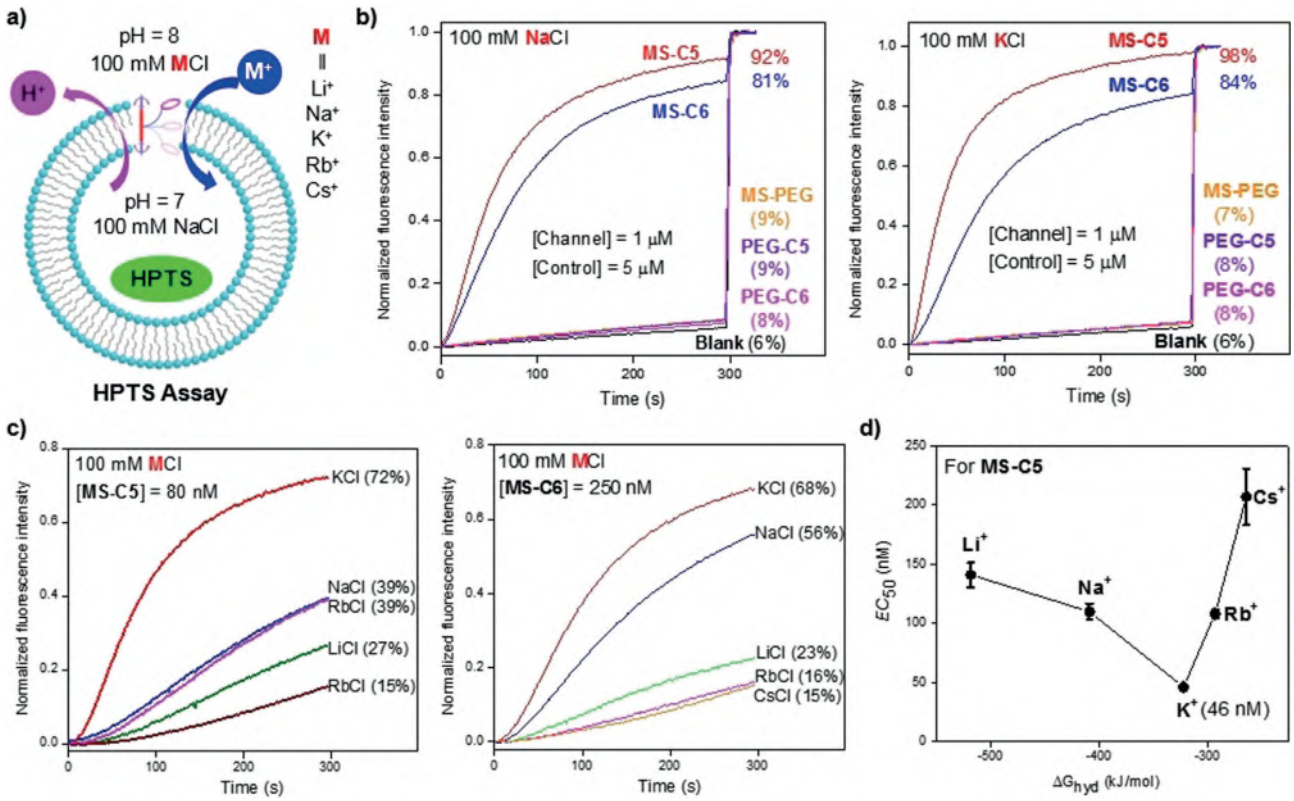

Figure 2. The pH-sensitive HPTS assay and measured ion-transport activities and selectivities for molecular swings **MS–C5** and **MS–C6**. a) Schematic illustration of the HPTS assay for evaluating ion-transport activities. b) Ion-transport activities of **MS–C5** and **MS–C6** at 1 μM and three control compounds **MS–PEG**, **PEG–C5**, and **PEG–C6** at 5 μM. c) Ion-transport selectivities of **MS-C5** at 80 nM and **MS-C6** at 250 nM. d) **MS–C5** EC_{50} values for the of transport alkali-metal ions.

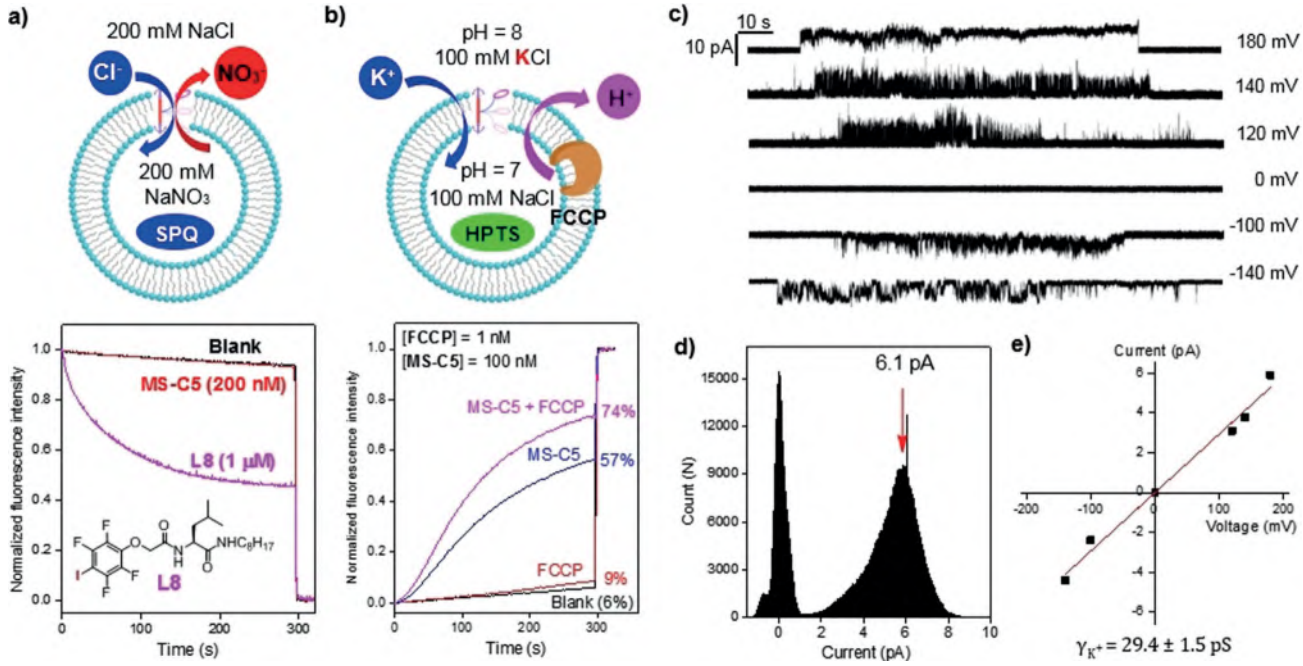

Figure 3. Deciphering the ion-transport mechanism and determined single-channel conductance value for **MS–C5**-mediated transport of K^+ ions. a) SPQ assay, demonstrating that **MS–C5** does not transport chloride anions. b) Carbonyl cyanide 4-(trifluoromethoxy) phenylhydrazone (**FCCP**)-based HPTS assay, showing that K^+ ions are transported faster than H^+ ions. c) Single-channel current traces recorded at various voltages in symmetric baths (*cis* chamber = *trans* chamber = 1 M KCl) for **MS–C5**. d) Point amplitude histogram for all the recorded digitized current values that gives a mean value of 6.1 pA at 180 mV. (For averaged current values and hitstograms at other voltages, see Figure S10 in the Supporting Information). e) Linear current–voltage (*I–V*) plot that yields a K^+ conductance value (γ_K) of 29.4 ± 1.5 pS for **MS–C5**.

ular KCl with NaCl produced similar results, similarly supporting that Na^+ is transported faster than H^+ (Supporting Information, Figure S9b).

As discussed above, molecular-swing-mediated ion transport follows a more defined pathway than a carrier, but more ill-defined than an ideal channel that exhibits only a single level conductance. To gain some insights into the mechanism (i.e., carrier or channel) by which the molecular swing transports K^+ ions, we recorded single-channel current traces in a planar lipid bilayer in symmetric baths (*cis* chamber = *trans* chamber = 1M KCl). The observation of single-channel current traces at various voltages unambiguously confirms that the molecular swing **MS–C5** behaves like a single channel in swinging ions across membrane (Figure 3c). As expected, numerous sublevel transitions do exist in these current traces. By plotting digitized current values vs. number of occurrences, point amplitude histograms were generated and used to obtain a mean current value (Figure 3d). Using these histograms, we obtained a mean value of 6.1 pA for channel currents recorded at 180 mV (Figure 3d; for mean values at other voltages, see Figure S10 in the Supporting Information). Linear fitting of current–voltage (*I–V*) curve gives a K^+ conductance value ($\gamma_K{}^+$) of 29.4 ± 1.5 pS (Figure 3E). This conductance value, which is 27% higher than that of gramicidin A (23.2 ± 0.4 pS) recently determined by us,[7b] corresponds to a highly efficient transport of 1.8×10^7 K^+ ions s^{-1} at 100 mV.

The highly efficient molecular-swing-mediated transmembrane transport of K^+ ions encouraged us to investigate possible uses of **MS–C5** and **MS–C6** in cancer chemotherapy. As the most aggressive primary brain tumor, glioblastoma expresses a variety of ion channels, with the expression level of the large conductance K^+ channels shown to positively correlate with the tumor malignancy grade.[8a] These K^+ channels are crucial in buffering extracellular K^+ ions for neuronal homeostasis as the over-accumulation of K^+ ions in the extracellular space results in depolarized neurons, which become less capable, or even incapable, of firing action potentials. Following a standard cell culturing protocol, the IC_{50} values of **MS–C5** and **MS–C6** toward a human primary glioblastoma cell line (U-87 MG, ATCC) were determined to be 60 ± 1.4 μM and 45 ± 0.6 μM, respectively (Supporting Information, Figure S11). This suggests significant anticancer activities of the molecular swings. In comparison, K^+ channel blockers, including quinidine, mostly display IC_{50} values of approximately 60 μM and above toward U-87 MG cell lines.[8b]

In summary, we have conceptually proposed and experimentally verified a novel molecular-machine-inspired swing mechanism for promoting highly efficient transmembrane flux of K^+ ions. While operating in a single-channel-like fashion, this class of molecular swings does not follow a single, well-defined ion permeation pathway. Instead, ion transport is mediated through numerous pathways, with an averaged performance in potassium transport that is 27% better than gramicidin A. Such highly active potassium transport helps to deliver good IC_{50} values of 60 and 45 μM for **MS–C5** and **MS–C6**, respectively, towards brain tumor cell line U-87 MG. Further structural optimizations might lead to higher anticancer activities. Given the currently available varied types of molecular machines with ranging and emerging functions, our strategy demonstrated here may capture the imagination and attention of others in creating a broad variety of motional channels with single-channel behaviors as well as high activity and selectivity in transmembrane transport. Besides breaking new grounds scientifically, these motional channels may lead to practical medical benefits in the future.

Acknowledgements

This work was supported by the Institute of Bioengineering and Nanotechnology and the NanoBio Lab (Biomedical Research Council, Agency for Science, Technology and Research, Singapore).

Conflict of interest

The authors declare no conflict of interest.

Keywords: molecular machine · molecular swing · supramolecular chemistry · synthetic ion channel

How to cite: *Angew. Chem. Int. Ed.* **2019**, *58*, 8034–8038
Angew. Chem. **2019**, *131*, 8118–8122

[1] a) J. T. Davis, O. Okunola, R. Quesada, *Chem. Soc. Rev.* **2010**, *39*, 3843–3862; b) P. R. Brotherhood, A. P. Davis, *Chem. Soc. Rev.* **2010**, *39*, 3633–3647; c) D. S. Kim, J. L. Sessler, *Chem. Soc. Rev.* **2015**, *44*, 532–546; d) S. Benz, M. Macchione, Q. Verolet, J. Mareda, N. Sakai, S. Matile, *J. Am. Chem. Soc.* **2016**, *138*, 9093–9096; e) P. A. Gale, J. T. Davis, R. Quesada, *Chem. Soc. Rev.* **2017**, *46*, 2497–2519.

[2] a) S. Matile, A. Vargas Jentzsch, J. Montenegro, A. Fin, *Chem. Soc. Rev.* **2011**, *40*, 2453–2474; b) A. Vargas Jentzsch, A. Hennig, J. Mareda, S. Matile, *Acc. Chem. Res.* **2013**, *46*, 2791–2800; c) J. Montenegro, M. R. Ghadiri, J. R. Granja, *Acc. Chem. Res.* **2013**, *46*, 2955–2965; d) T. M. Fyles, *Acc. Chem. Res.* **2013**, *46*, 2847–2855; e) F. Otis, M. Auger, N. Voyer, *Acc. Chem. Res.* **2013**, *46*, 2934–2943; f) G. W. Gokel, S. Negin, *Acc. Chem. Res.* **2013**, *46*, 2824–2833; g) M. Barboiu, A. Gilles, *Acc. Chem. Res.* **2013**, *46*, 2814–2823; h) B. Gong, Z. Shao, *Acc. Chem. Res.* **2013**, *46*, 2856–2866; i) W. Si, P. Xin, Z.-T. Li, J.-L. Hou, *Acc. Chem. Res.* **2015**, *48*, 1612–1619; j) Y. P. Huo, H. Q. Zeng, *Acc. Chem. Res.* **2016**, *49*, 922–930.

[3] a) G. S. Kottas, L. I. Clarke, D. Horinek, J. Michl, *Chem. Rev.* **2005**, *105*, 1281–1376; b) W. R. Browne, B. L. Feringa, *Nat. Nanotechnol.* **2006**, *1*, 25; c) J. Berná, D. A. Leigh, M. Lubomska, S. M. Mendoza, E. M. Pérez, P. Rudolf, G. Teobaldi, F. Zerbetto, *Nat. Mater.* **2005**, *4*, 704; d) J. Bath, A. J. Turberfield, *Nat. Nanotechnol.* **2007**, *2*, 275; e) V. Balzani, A. Credi, M. Venturi, *Chem. Soc. Rev.* **2009**, *38*, 1542–1550; f) A. Coskun, M. Banaszak, R. D. Astumian, J. F. Stoddart, B. A. Grzybowski, *Chem. Soc. Rev.* **2012**, *41*, 19–30; g) S. Erbas-Cakmak, D. A. Leigh, C. T. McTernan, A. L. Nussbaumer, *Chem. Rev.* **2015**, *115*, 10081–10206; h) K. Hermann, Y. Ruan, A. M. Hardin, C. M. Hadad, J. D. Badjić, *Chem. Soc. Rev.* **2015**, *44*, 500–514; i) C. Pezzato, C. Cheng, J. F. Stoddart, R. D. Astumian, *Chem. Soc. Rev.* **2017**, *46*, 5491–5507; j) S. Kassem, T. van Leeuwen, A. S. Lubbe, M. R. Wilson, B. L. Feringa, D. A. Leigh, *Chem. Soc. Rev.* **2017**, *46*, 2592–2621; k) J. H. van Esch, R. Klajn, S. Otto, *Chem. Soc. Rev.* **2017**, *46*, 5474–5475; l) J. D. Harris, M. J. Moran, I. Aprahamian, *Proc. Natl. Acad. Sci. USA* **2018**, *115*, 9414–9422.

[4] a) J.-P. Sauvage, *Angew. Chem. Int. Ed.* **2017**, *56*, 11080 – 11093; *Angew. Chem.* **2017**, *129*, 11228 – 11242; b) J. F. Stoddart, *Angew. Chem. Int. Ed.* **2017**, *56*, 11094 – 11125; *Angew. Chem.* **2017**, *129*, 11244 – 11277; c) B. L. Feringa, *Angew. Chem. Int. Ed.* **2017**, *56*, 11060 – 11078; *Angew. Chem.* **2017**, *129*, 11206 – 11226.

[5] a) R. Eelkema, M. M. Pollard, J. Vicario, N. Katsonis, B. S. Ramon, C. W. M. Bastiaansen, D. J. Broer, B. L. Feringa, *Nature* **2006**, *440*, 163; b) L. Greb, J.-M. Lehn, *J. Am. Chem. Soc.* **2014**, *136*, 13114 – 13117; c) Q. Li, G. Fuks, E. Moulin, M. Maaloum, M. Rawiso, I. Kulic, J. T. Foy, N. Giuseppone, *Nat. Nanotechnol.* **2015**, *10*, 161; d) M. R. Wilson, J. Solà, A. Carlone, S. M. Goldup, N. Lebrasseur, D. A. Leigh, *Nature* **2016**, *534*, 235; e) S. Erbas-Cakmak, S. D. P. Fielden, U. Karaca, D. A. Leigh, C. T. McTernan, D. J. Tetlow, M. R. Wilson, *Science* **2017**, *358*, 340 – 343; f) P. Thordarson, E. J. A. Bijsterveld, A. E. Rowan, R. J. M. Nolte, *Nature* **2003**, *424*, 915; g) B. Lewandowski, G. De Bo, J. W. Ward, M. Papmeyer, S. Kuschel, M. J. Aldegunde, P. M. E. Gramlich, D. Heckmann, S. M. Goldup, D. M. D'Souza, A. E. Fernandes, D. A. Leigh, *Science* **2013**, *339*, 189 – 193; h) V. Serreli, C.-F. Lee, E. R. Kay, D. A. Leigh, *Nature* **2007**, *445*, 523; i) C. Cheng, P. R. McGonigal, S. T. Schneebeli, H. Li, N. A. Vermeulen, C. Ke, J. F. Stoddart, *Nat. Nanotechnol.* **2015**, *10*, 547; j) M. C. Jiménez, C. Dietrich-Buchecker, J.-P. Sauvage, *Angew. Chem. Int. Ed.* **2000**, *39*, 3284 – 3287; *Angew. Chem.* **2000**, *112*, 3422 – 3425; k) C. J. Bruns, J. F. Stoddart, *Acc. Chem. Res.* **2014**, *47*, 2186 – 2199; l) M. von Delius, E. M. Geertsema, D. A. Leigh, *Nat. Chem.* **2009**, *2*, 96; m) S. Kassem, A. T. L. Lee, D. A. Leigh, A. Markevicius, J. Solà, *Nat. Chem.* **2015**, *8*, 138.

[6] S. Chen, Y. Wang, T. Nie, C. Bao, C. Wang, T. Xu, Q. Lin, D.-H. Qu, X. Gong, Y. Yang, L. Zhu, H. Tian, *J. Am. Chem. Soc.* **2018**, *140*, 17992 – 17998.

[7] a) H. Q. Zhao, S. Sheng, Y. H. Hong, H. Q. Zeng, *J. Am. Chem. Soc.* **2014**, *136*, 14270 – 14276; b) C. L. Ren, J. Shen, H. Q. Zeng, *J. Am. Chem. Soc.* **2017**, *139*, 12338 – 12341; c) C. L. Ren, X. Ding, A. Roy, J. Shen, S. Zhou, F. Chen, S. F. Yau Li, H. Ren, Y. Y. Yang, H. Q. Zeng, *Chem. Sci.* **2018**, *9*, 4044 – 4051; d) C. L. Ren, F. Zeng, J. Shen, F. Chen, A. Roy, S. Zhou, H. Ren, H. Q. Zeng, *J. Am. Chem. Soc.* **2018**, *140*, 8817 – 8826.

[8] a) R. J. Molenaar, *ISRN Neurol.* **2011**, *2011*, 590249; b) Q. Ru, X. Tian, M. S. Pi, L. Chen, K. Yue, Q. Xiong, B. M. Ma, C. Y. Li, *Int. J. Oncol.* **2015**, *46*, 833 – 840.

Manuscript received: February 12, 2019
Accepted manuscript online: April 14, 2019
Version of record online: May 8, 2019

